

# $^{16}\text{O}$ within the Semimicroscopic Algebraic Cluster Model and the importance of the Pauli Exclusion Principle

P. O. Hess<sup>1,2</sup>, J. R. M. Berriel-Aguayo<sup>1</sup> and L. J. Chávez-Nuez<sup>1</sup>

<sup>1</sup> Instituto de Ciencias Nucleares, Universidad Nacional Autónoma de México, Ciudad Universitaria, Circuito Exterior S/N, A.P. 70-543, 04510 México D.F. México e-mail: [hess@nucleares.unam.mx](mailto:hess@nucleares.unam.mx)

<sup>2</sup> Frankfurt Institute for Advanced Studies, Johann Wolfgang Goethe Universität, Ruth-Moufang-Str.1, 60438 Frankfurt am Main, Germany

Received: date / Revised version: date

**Abstract.** The *Semimicroscopic Algebraic Cluster Model* (SACM) is applied to  $^{16}\text{O}$ , assumed to consist of a system of four  $\alpha$ -clusters. For the  $4\alpha$  cluster system a microscopic model space is constructed, which observes the *Pauli-Exclusion-Principle* (PEP) and is symmetric under permutation of the  $4\alpha$ -particles. A phenomenological Hamiltonian is used, justifying the name *Semi* in the SACM. The spectrum and transition values are determined. One of the main objectives is to test the importance of the *Pauli Exclusion Principle* (PEP), comparing the results with the *Algebraic Cluster Model* (ACM), which does not include the PEP, and claims that the  $^{16}\text{O}$  shows evidence of a tetrahedral structure, which can be explained easily by symmetry arguments. We show that PEP is very important and cannot be neglected, otherwise it leads to a wrong interpretation of the band structure and to too many states at low energy.

**Key words.** nuclear clusters, algebraic model, Pauli Principle

**PACS.** 21. Nuclear structure – 21.60.Gx Cluster models – 21.10.Re Collective levels

## 1 Introduction

$^{16}\text{O}$  nucleus is a test case for many structural investigations, as for example microscopic full scale calculations [1, 2], study of  $\alpha$ -cluster condensation [3,4,5]. Reviews are published in [4,6,7,8] and still open problems are discussed in [9,10]. All of them use the PEP as a fundamental principle. In [11,12] the *Algebraic Cluster Model* (ACM) is applied to  $^{16}\text{O}$ , not taking into account the PEP. The claim is that experimental information supports a tetrahedral structure of  $^{16}\text{O}$  in its ground and excited states. The spectrum and several electromagnetic transition values are calculated and the agreement to experiment seems acceptable.

The similar claim was made in [13,14] for the  $^{12}\text{C}$  nucleus having a triangular structure. Experimental data seems to be well reproduced. In [13] the additional measured  $5^-$  state was argued as an evidence for the triangular structure.

In [15] the  $^{12}\text{C}$  nucleus was reexamined, within the SACM [16,17], with the same objective as here, namely to investigate the importance of the PEP and changes in structure when it is taken into account. The main finding was that the spectrum and transition values can be equally reproduced as in [14], in fact there are several procedures which can (see e.g. [6]). It was shown that PEP is important: Not taking into account the PEP leads to too many

states at low energy, the association into bands as done in [14] is wrong, not supported by the shell model, and the geometrical interpretation is trivial. The measured  $5^-$  state [13] is not an evidence for the triangular structure, and in addition, a further  $5^-$  state predicted by the ACM at low energy is not supported by the shell model. Using the symmetry character of the  $\alpha$  particles under permutation, in the ground state the configuration has to be a triangle, however not necessarily for the excited states, as for the Hoyle state [18].

In this contribution we investigate if the claims in [11, 12] are justified. We will use again the *Semimicroscopic Algebraic Cluster Model* [16,17], whose model space observes the PEP but whose Hamiltonian is phenomenological. The advantage of this model is its easy application, allowing large scale calculations (complete spectrum and transition values), and its similarity to the model used in [11,12]. We will concentrate on the energies,  $B(EL)$  ( $L = 2, 3$ ) values for making a point, namely that the ACM is inconsistent in not taking into account the PEP. The calculation of more experimental data does not improve the situation.

In section 2 the model space of  $^{16}\text{O}$  is constructed, in section 3 the Hamiltonian presented and results are shown. In section 4 Conclusions are drawn.

## 2 The model space for $^{16}\text{O}$

In this section the SACM model space is constructed for a completely symmetric  $4-\alpha$  particle system, satisfying the PEP. The procedure can be reduced to a pure counting, avoiding cumbersome calculations of kernels. We construct *ket*-states, classified by their quantum numbers.

In a system of four identical particles, 3 Jacobi coordinate vectors are introduced, leading to invariance in spatial translations:

$$\begin{aligned} \boldsymbol{\lambda}_1 &= \frac{1}{\sqrt{2}}(\mathbf{x}_2 - \mathbf{x}_1) \\ \boldsymbol{\lambda}_2 &= \frac{1}{\sqrt{6}}(2\mathbf{x}_3 - \mathbf{x}_1 - \mathbf{x}_2) \\ \boldsymbol{\lambda}_3 &= \frac{1}{\sqrt{12}}(3\mathbf{x}_4 - \mathbf{x}_1 - \mathbf{x}_2 - \mathbf{x}_3) \quad , \end{aligned} \quad (1)$$

where  $\mathbf{x}_k$  denotes the position vector of the  $k$ 'th particle. The first one,  $\boldsymbol{\lambda}_1$ , is the relative vector between the first two particles, the second one,  $\boldsymbol{\lambda}_2$ , is a vector from the third particle to the center of mass of the first two and the last Jacobi vector,  $\boldsymbol{\lambda}_3$ , connects the fourth particle to the center of mass of the first three. For each of the Jacobi vectors we can associate an harmonic oscillator, with quantum numbers  $(N_{\lambda_k}, l_{\lambda_k}, m_{\lambda_k})$ ,  $N_{\lambda_k}$  being the number of oscillation quanta,  $l_{\lambda_k}$  is the angular momentum and  $m_{\lambda_k}$  is its projection. For each of the sub-systems the Wildermuth condition [19] has to be satisfied. The Wildermuth condition gives the minimal number of relative oscillation quanta, necessary for observing the PEP. In the case of  $^{16}\text{O}$ , for the two-particle sub-system the minimal number of quanta is 4, the same for the second and the third oscillator.

The definition (1) does not consider that the four particle state has to be symmetric under permutation, thus one can use also any other combination for the Jacobi coordinates, permuting the indices. In order to do so, in what follows we indicate the construction of completely symmetric states, which however does not yet include the Wildermuth condition. This will be done in a subsequent step.

In [20] the states for 4 identical particles was constructed for an arbitrary permutation symmetry, while in [21] the basic method is explained, though only angular momentum zero states were considered. Here, we outline the basic steps, for a complete symmetric system:

New coordinates were defined in [20], i.e.,

$$\begin{aligned} \ddot{\mathbf{x}}^1 &= (\mathbf{x}^1 + \mathbf{x}^4 - \mathbf{x}^2 - \mathbf{x}^3) \\ \ddot{\mathbf{x}}^2 &= (\mathbf{x}^2 + \mathbf{x}^4 - \mathbf{x}^1 - \mathbf{x}^3) \\ \ddot{\mathbf{x}}^3 &= (\mathbf{x}^3 + \mathbf{x}^4 - \mathbf{x}^1 - \mathbf{x}^2) \quad , \end{aligned} \quad (2)$$

which have more useful properties under permutation.

The  $S_4$  permutation group can be written as a semi-direct product  $D_2 \wedge S_3$ , where the  $D_2$  is composed of the permutations

$$\begin{aligned} e, \quad d_1 &= (1, 4)(2, 3), \quad d_2 = (2, 4)(1, 3), \\ d_3 &= (3, 4)(1, 2) \quad , \end{aligned} \quad (3)$$

where  $(i, j)$  denotes the permutation of  $i$  with  $j$  and  $e$  is the unit element. The  $S_3$  is the permutation group of the first three coordinates  $\mathbf{x}^1, \mathbf{x}^2$  and  $\mathbf{x}^3$ . A general permutation can be written as the product of an element of  $D_2$  with  $S_3$ .

Restricting to a complete symmetric state (as it is the case for a  $4-\alpha$  system), the state will be multiplied by the factor [20]

$$\left( 1 + (-1)^{\ddot{l}_1 + \ddot{l}_2} + (-1)^{\ddot{l}_1 + \ddot{l}_3} + (-1)^{\ddot{l}_2 + \ddot{l}_3} \right) \quad , \quad (4)$$

where  $\ddot{l}_k$  is the orbital angular momentum of the oscillator basis state. This factor is only different from zero, if all  $\ddot{l}_k$  are even or odd. This also implies that the oscillation quantum numbers  $\ddot{N}_k$  (related to the coordinate  $\ddot{\mathbf{x}}^k$ ) have to be either all even or all odd.

The general expression for the basis state is

$$| \left[ (\ddot{N}_1 \ddot{l}_1, \ddot{N}_2 \ddot{l}_2) l_{12}; \ddot{N}_3 \ddot{l}_3 \right] \rho(\lambda\mu) \kappa LM \rangle \quad . \quad (5)$$

A state with  $\ddot{N}_k$  oscillation quanta transforms as  $(\ddot{N}_k, 0)$  with respect to  $SU(3)$ ,  $(\lambda, \mu)$  is a general  $SU(3)$  irreducible representation (irrep),  $\rho$  and  $\kappa$  is a multiplicity indices,  $l_{12}$  the intermediate angular momentum to which the first two oscillator functions are coupled,  $L$  is the total angular momentum and  $M$  its projection. In order to avoid a double counting, an order has to be followed. One possibility is to use

$$\ddot{N}_1 \geq \ddot{N}_2 \geq \ddot{N}_3 \quad . \quad (6)$$

Thus the preliminary list of  $SU(3)$  irreps for a 4-particle system is obtained by multiplying  $(\ddot{N}_1, 0) \otimes (\ddot{N}_2, 0) \otimes (\ddot{N}_3, 0)$ , with the order given in (6),  $\ddot{N}_1 + \ddot{N}_2 + \ddot{N}_3 = N$ ,  $N$  being the number of oscillation quanta in the system considered and taking into account that when  $N$  is even (odd), also all  $\ddot{N}_k$  have to be even (odd) [20]. Another restriction enters when  $(\ddot{N}_1, 0)$  is coupled with  $(\ddot{N}_2, 0)$  to certain  $SU(3)$  irreps  $(\lambda, \mu)$ : For  $\ddot{N}_1 = \ddot{N}_2$ , the  $SU(3)$  Clebsch-Gordan coefficient involved requires by symmetry that  $\lambda + \mu = \text{even}$ .

In such a manner, for each number of total oscillation quanta,  $N$ , a list of  $SU(3)$  irreps  $(\lambda\mu)$  and their multiplicity  $\rho$  of appearance is obtained.

This list still contains too many irreps. One has to subtract from it all irreps which violate the *Wildermuth condition* [19] and we determine it in the following:

First, we have  $N_{\lambda_1} + N_{\lambda_2} + N_{\lambda_3} = N$ , with  $N_{\lambda_1} \leq N_{\lambda_2} \leq N_{\lambda_3}$ . The coupling of  $(N_{\lambda_1}, 0)$  with  $(N_{\lambda_2}, 0)$ , for  $N_{\lambda_1} = N_{\lambda_2}$ , underlies the same symmetry restriction, as discussed above. Each combination of the  $N_{\lambda_k}$ , where at

least one of the  $N_{\lambda_k}$  is lower than allowed by the Wildermuth condition, provides a condition for which the state has to vanish. Thus, if a given  $SU(3)$  irrep,  $(\lambda, \mu)$  appear with a multiplicity  $\rho$  in the list of completely symmetric states, each single condition of a not allowed combination of the  $N_{\lambda_k}$  reduces this multiplicity by one. There may be more conditions for the same  $(\lambda, \mu)$ . If there are  $\delta$  of those conditions, the final multiplicity of the  $(\lambda, \mu)$  irrep is  $(\rho - \delta)$ . If this number is lower or equal to zero, the irrep in question is skipped completely from the list.

The procedure just explained provides a list of  $SU(3)$  irreps for a given excitation number  $\Delta n_\pi$ , having already taken into account the Wildermuth condition as a minimal one for observing the PEP. However, this list still contains irreps which are not allowed by the Pauli exclusion principle. For example, for  $\Delta n_\pi = 0$ , one obtains by the above explained procedure the (2,2), (1,1) and (0,0) irreps, from which only the last one is permitted. The final step is to apply the method of the SACM and look at the *overlap* of the list with shell model states. We will only consider states of the so-called *super-multiplets* [22]. A super-multiplet is characterized by the "most antisymmetric" irreducible representation (irrep) of the spin-isospin  $U(4)$  group, i.e. for a system of  $4n$  particles, it is of the form  $[n^4]$ , for  $(4n + 1)$  it is  $[5, 4^n]$ , etc., they correspond for  $4n$  particles to spin-isospin zero states. To be more specific, considering a particular shell number  $\eta$  with an occupation number  $A_\eta$ . The relevant group chain for classification is

$$U\left(4 * \frac{1}{2}(\eta + 1)(\eta + 2)\right) \supset U\left(\frac{1}{2}(\eta + 1)(\eta + 2)\right) \otimes_{UST} U(4) \quad (7)$$

$$\begin{array}{ccc} [1^{A_\eta}] & [\tilde{h}] & [h] \end{array}$$

where  $[h]$  is the Young diagram of the  $U(4)$  group and  $[\tilde{h}]$  the conjugate diagram, where rows and columns are interchanged. The  $S$  and  $T$  refer to spin and isospin quantum number respectively. The  $SU(3)$  group is contained in the orbital group  $U\left(\frac{1}{2}(\eta + 1)(\eta + 2)\right)$ , i.e., in order to get the shell model content one has to apply a reduction. Programs for that are available [23,24]. In a standard manner the center of mass spurious motion is subtracted.

With that, we are lead to the list of  $SU(3)$  irreps as given in Table 1, for up to 4 excited quanta.

Already from Table 1 the grouping of states into bands can be deduced within a pure  $SU(3)$  symmetry (see also [25]): Each band is classified by their  $SU(3)$  irrep  $(\lambda, \mu)$ . As shown in [26,27], the quadrupole deformation associated to each irrep is given by

$$\beta = \left[ \left( \frac{4\pi}{2N_s^2} \right) (\lambda^2 + \lambda\mu + \mu^2 + 3\lambda + 3\mu) \right]^{\frac{1}{2}} \quad (8)$$

The deformations for the (0,0) is 0, for (3,1) it is 0.36 and for (4,2) it is 0.49, i.e., each irrep has a completely different deformation and, thus, defining a different band.

| $n\hbar\omega$ | $(\lambda, \mu)$   |
|----------------|--|
| 0              | (0,0)  |
| 1              | (2,1)  |
| 2              | (2,0), (3,1), (4,2)  |
| 3              | (3,0), (4,1), (1,4), (5,2), (6,3)  |
| 4              | (0,2), (1,3), (4,0) <sup>2</sup> , (3,2) <sup>2</sup> , (2,4), (5,1) <sup>3</sup> , (4,3), (3,5), (6,2) <sup>2</sup> , (7,3) |

**Table 1.** Model space of the 4- $\alpha$ -particle system, for up to  $4\hbar\omega$  excitations and only including states with the "most antisymmetric" irrep in  $U_{ST}(4)$ . Multiplicities larger than 1 are indicated by an upper index.

## 3 The Hamiltonian and

### 3.1 The Hamiltonian

As a Hamiltonian we propose a combination of a pure  $SU(3)$ -part and a symmetry breaking term, which is a generator of  $SO(4)$ . There are more general ones, but we want to keep it simple enough with the number of parameters as in [12]. The choice does not exclude more general Hamiltonians. As in [11] the total number of quanta is  $N = n_{\lambda_1} + n_{\lambda_2} + n_{\lambda_3} + n_\sigma = n_\pi + n_\sigma$ , where the  $\sigma$ -bosons are introduced as a trick to obtain a cut-off and  $n_\pi$  refers here to the total number of excited quanta in the relative motion. The  $\pi_m^\dagger$ -boson operators ( $m = 0, \pm 1$ ) are the creation and the  $\pi^m$  operators are the annihilation operators for the total relative motion. The algebra is  $U(3)$  and their generators  $C_m^{m'}$  are the sum of generators of the three harmonic oscillators related to the Jacobi coordinates.

For  $^{16}\text{O}$ , the model Hamiltonian proposed is

$$\begin{aligned} H = & \hbar\omega n_\pi - \chi (1 - \xi \Delta n_\pi) \mathbf{C}_2(\lambda, \mu) + t_1 \mathbf{C}_3(\lambda, \mu) \\ & + t_2 (\mathbf{C}_2(\lambda, \mu))^2 + (a + a_{Lnp} \Delta n_\pi) \mathbf{L}^2 + b \mathbf{K}^2 \\ & + b_1 \left[ (\boldsymbol{\sigma}^\dagger)^2 - (\boldsymbol{\pi}^\dagger \cdot \boldsymbol{\pi}^\dagger) \right] \cdot [h.c.] \quad (9) \end{aligned}$$

The first term is just the harmonic oscillator field and the  $\hbar\omega$  is fixed via  $45 \times A^{-1/3} - 25 \times A^{-2/3}$  [28] (units in MeV), where its value is 13.92 MeV for  $^{16}\text{O}$ . The second term is proportional to the quadrupole-quadrupole interaction. The intensity of this interaction is modified with increasing shell model excitation. The third term is the third-order Casimir operator, which allows to distinguish between  $(\lambda, \mu)$  and  $(\mu, \lambda)$ . In the second line, the first term is the square of the second-order Casimir operator of  $SU(3)$ . The second term is the  $\mathbf{L}^2$  term. The factor describes changes in the moment of inertia as a function of the shell excitation. The third term distinguishes between angular momentum states in the same  $SU(3)$  irrep. Finally, the last line contains the  $SU(3)$ - $SO(4)$  mixing interaction.

Up to the second line, the Hamiltonian is within the  $SU(3)$  limit and permits analytic results, substituting the operators by their corresponding eigenvalues. The term in the last line mixes  $SU(3)$  irreps, it is a generator of a  $SO(4)$  group. The pure  $SU(3)$  part has 7 free parameters

and including the  $b_1$ , corresponding to  $SO(4)$  mixture, there are in total 8 parameters. This is the same number as in the  $^{12}\text{C}$  case [15]. As we will see in the applications, the fits require  $a = 0$ , so in fact there is one parameter less.

The physical quadrupole operator [29,30] is given by

$$\begin{aligned} Q_{2m}^{phys} &= Q_{2m}^a + \frac{\sqrt{6}}{2} (B_{2m}^\dagger + B_{2m}) \\ B_{2m}^\dagger &= (\pi^\dagger \cdot \pi^\dagger) , \quad B_{2m} = (\pi \cdot \pi) \\ Q_{2m}^a &= \sqrt{6} [\pi^\dagger \otimes \pi]_m^2 \quad . \end{aligned} \quad (10)$$

The  $B_{2m}^\dagger$  operator transforms as a  $(2,0)$   $SU(3)$  irrep, while  $B_{2m}$  as its conjugate.

### 3.2 Remarks on a geometrical mapping

In [15] a geometrical mapping of the Hamiltonian for the  $^{12}\text{C}$  nucleus was presented. The main steps [31] are to define a trial state  $|\alpha\rangle$  and the classical potential as the expectation value of the Hamiltonian with respect to this trial state, i.e., [31]

$$V(\alpha) = \langle \alpha | H | \alpha \rangle \quad . \quad (11)$$

In the case of  $^{12}\text{C}$  it was found that in the ground state by default a triangular structure of the three- $\alpha$  particle system has to be realized. The argument relies on the fact that the  $\alpha$ -particles are indistinguishable and the distance of the first to the second particle has thus to be equal as the distance of the first to the third and the second to the third particle. One has to keep in mind that the notion of "first", "second" and "third" does not make sense due to the indistinguishability of the  $\alpha$ -particles, it is only a *classical* picture.

The same can be applied to the  $^{16}\text{O}$  nucleus as a system of four  $\alpha$ -particles: The distance of any two  $\alpha$ -particle has to be the same. The only geometrical figure, which satisfies it, is the tetrahedral structure.

The situation changes when excited states are considered, which allows the mixing of different geometrical configurations and as a result the tetrahedral structure is lost in general.

The important point is that even when the density profiles show a tetrahedral structure (see for example [32]) and a *classical* description of this symmetry leads to a classification according to the  $T_4$  dynamical group, the projection of these *classical* wave functions onto antisymmetrized states leads to destroy the association into bands according to  $T_4$ . For example, antisymmetrization of the ground state leads to a spherical nucleus and the band associated to it consists only of one and one state.

To resume, the methods used in atomic molecular physics cannot be translated without cause to nuclear physics, where the PEP plays an essential role. In atomic molecular physics there is no overlap of the wave function between each atom nucleus but in nuclear physics there is.

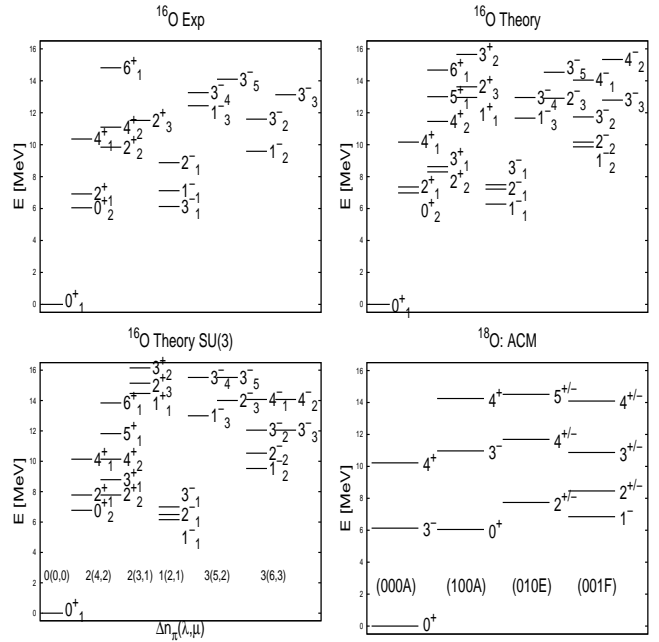


**Fig. 1.** Spectrum of  $^{16}\text{O}$ . The left panel in the first row is the experimental spectrum and the right one depicts the result of the theory. Experimental data are taken from [33]. In the lower row, the left panel depicts the result for the  $SU(3)$  limit while the right figure shows the result of Ref. [12], with the ordering of bands as done in [12]. The figure contains less bands than shown in the other figures.

### 3.3 Results

In Fig. 1, on the left panel in the upper row the experimental spectrum is depicted and the right hand figure in the first row the theoretical spectrum, as obtained by our fit. In the lower row, left side, the result for the  $SU(3)$  limit is given and the last panel shows the result of [12]. There, the bands are ordered as done in [12] and it contains less bands than listed in the other figures.

The agreement of the theoretical spectrum to the experimental one is satisfactory. The difference to the  $SU(3)$  limit is minor, mainly the degeneracy between the two lowest  $4^+$  states is lifted. Comparing the  $SU(3)$  limit with the calculation with mixing, the spectra look very similar. Inspecting Table 2 one also notes that the mixing term  $b_1$  is very small. Another feature is that the  $a$ -parameter is zero, only the  $a_{Lnp}$ -parameter remains and it is positive. This again illustrates that the  $^{16}\text{O}$  nucleus is spherical, with the ground state band consisting only of the  $0_1^+$  state. The excited states already belong to shell excitations ( $\Delta n_\pi > 0$ ), the nucleus gets deformed and can rotate ( $a_{Lnp} \neq 0$ ).

The energy spectrum in [12] is obtained with the formula

$$\Delta E = \omega_1 v_1 + \omega_2 v_2 + \omega_3 v_3 + B_{[v]} L(L+1) \quad , \quad (12)$$

where  $v_k = 0, 1, \dots$  are the quantum numbers of the model and  $B_{[v]}$  ( $[v] = v_1 v_2, v_3$ ) is the parameter to adjust for each



| param. [MeV] | Theo.     | $SU(3)$    |
|--------------|-----------|------------|
| $\chi$       | 0.41263   | 0.46007    |
| $\xi$        | 0.26145   | 0.072041   |
| $t_1$        | -0.030068 | -0.019610  |
| $t_2$        | 0.0072660 | 0.00413550 |
| $a$          | 0.        | 0.         |
| $a_{Lnp}$    | 0.091400  | 0.0841543  |
| $b$          | -0.1998   | 0.         |
| $b_1$        | -0.051895 | 0.         |
| $pe_2$       | 0.53112   | 0.33189    |

**Table 2.** List of the parameter values used. The first column lists the parameter symbols, the second their numerical value for the theoretical fit, including the  $b_1$  term. The third list are the parameters in the  $SU(3)$  limit. Note the small  $b_1$  parameter, which indicates a very small mixing to  $SO(4)$ .

| $B(EL; J_i^\pi \rightarrow J_f^\pi)$ | EXP.           | theo  | $SU(3)$ | Ref. [12] |
|--------------------------------------|----------------|-------|---------|-----------|
| $B(E2; 2_1^+ \rightarrow 0_1^+)$     | $3.1 \pm 0.1$  | 0.003 | 0.0     | 10.9      |
| $B(E2; 2_1^+ \rightarrow 0_2^+)$     | $27.0 \pm 3.0$ | 18.55 | 2.52    | 2.50      |
| $B(E2; 4_1^+ \rightarrow 2_1^+)$     | $65. \pm 6.0$  | 0.06  | 0.62    | -         |
| $B(E2; 4_2^+ \rightarrow 2_1^+)$     | $1. \pm 5.0$   | 0.21  | 1.26    | 15.0      |
| $B(E2; 1_1^- \rightarrow 3_1^-)$     | $21. \pm 5.0$  | 0.    | 0.0     | 7.93      |
| $B(E2; 2_1^- \rightarrow 1_1^-)$     | $10.3 \pm 0.1$ | 11.16 | 4.36    | 3.34      |
| $B(E2; 2_1^- \rightarrow 3_1^-)$     | $8.2 \pm 3.0$  | 11.56 | 4.52    | 4.18      |
| $B(E3; 3_1^- \rightarrow 0_1^+)$     | $13.5 \pm 0.7$ | 20.08 | 21.45   | 5.27      |

**Table 3.** List of  $B(EL)$ -transition values, measured and obtained in three different model calculations: In the first column information is listed on the type of the electromagnetic transition, the second column lists the corresponding experimental values, the third column corresponds to the theoretical calculations with the  $b_1$  term and the fourth column lists the values in the  $SU(3)$  limit. The last column lists the values as obtained in [12].

band the moment of inertia. Four bands are considered: (000A), (100A), (010E) and (001F). The parameter values used are  $\omega_k = 6.05\text{MeV}$  ( $k = 1, 2, 3$ ),  $B_{000A} = 0.511\text{MeV}$ ,  $B_{100A} = 0.410\text{MeV}$ ,  $B_{010E} = 0.282\text{MeV}$  and  $B_{001F} = 0.420\text{MeV}$ . With this choice the spectrum depicted in Fig. 1 on the right in the lower row is reproduced. Note, that the formula (12) consists of *linear independent parameters*, which allow to adjust the states within any band and, thus, is not of great predictive power. On the other hand, in the SACM the parameters are interconnected to all bands and thus are not linear independent, changing one parameter has an effect on all bands.

In Table 3 some  $B(EL)$  transition values are listed and compared to experiment. As can be seen, the  $B(E2)$ -values, which are a good measure for the structure of the wave functions, are well reproduced and often better than in the ACM [12]. We use a geometrical estimation of the effective charges, as explained in [34]. For the octupole transition no additional fitting is used, while for the  $B(E2)$ -transitions one global factor is adjusted. If this factor is near to the value of 1, it is an indication that the geometrical estimation is quite good. As shown in [34] the geometric estimate of the effective charge is multiplied by

a parameter  $pe_2$  ( $\sim \beta^6$  [12]) in the quadrupole operator. Consulting Table 2, the  $pe_2$  is approximately 0.53, which indicates a rather good estimation. The  $B(E3; 3_1^- \rightarrow 0_1^+)$ -value is reproduced in order, but when the scaling factor  $\sim \beta^8$  [12] for the  $B(E3)$  is applied, this value reduces to 8.63, which is in quite good agreement to experiment. For the calculation of this value an octupole deformation for the  $3_1^-$  state was needed as an input. This value is estimated within the geometrical model [35] and given in the Appendix. In order to have a better test of a model, one also has to compare various  $B(E3)$  and  $B(E4)$  values to experiment and not just one. For our purposes this is not necessary, because it is sufficient to show if the PEP already leads in the spectrum to clear structural differences to the ACM.

In Tables 4 and 5 we list the content of some of the states in the spectrum in order to show that one can group them into bands. Shown is the percent contribution of a state to a given  $n_\pi(\lambda, \mu)$ : If a state belongs to the same band, the distribution has to be similar! As can be seen, the  $0_1^+$  state is the only state of a "band", it is a hundred percent pure (0,0). These tables also show that all states are practically pure  $SU(3)$  states, demonstrating that the  $^{16}\text{O}$  is a show-case for the  $SU(3)$  shell model. There are some small admixtures to other  $SU(3)$  irreps, but the numbers listed are rounded off, such that e.g. 99.8 percent is shown as a 100 percent contribution.

One notes that the grouping into bands has nothing to do with the one defined in [12]. In order to associate states to the same band, the internal structure has to be the same (at least approximately with mixing). The ground state belongs to the (0,0)  $SU(3)$  irrep and 12 oscillation quanta, thus it is the *only* representative of the band. The other bands are ordered according to the membership to  $SU(3)$  irreps and different irreps have distinct deformations. It is clear that this ordering into bands does not agree at all with [12], where a pure classical picture of the nucleus was assumed and the  $\alpha$ -particles with no internal structure. The association into bands is maintained when mixing is included.

The experimental data can be reproduced better within the SACM (see Table 3). The spectrum can be reproduced equally well to the already existing data. However, comparing the complete spectrum of both theories leads to significant differences between the SACM and [12]: Not considering the PEP leads to a denser spectrum, which is lifted in the SACM. The multiplets reported in the (010E) and (001F) bands (see Fig. 1 [12]) are not there. Only the search for a more complete spectrum can show the differences. The association into bands is easier in  $^{16}\text{O}$  than in  $^{12}\text{C}$  [15], because the states are each concentrated in practically one  $SU(3)$  irrep.

## 4 Conclusions

The structure of  $^{16}\text{O}$  in terms of a 4- $\alpha$  particle system within the SACM and the importance of the PEP was investigated, comparing it to [12] where the PEP was ignored. It is shown that in the ground state a tetrahedral

| $n\hbar\omega (\lambda, \mu) / L_i^\pi$ | $0_1^+$ | $2_1^+$ | $4_1^+$ | $0_2^+$ | $2_2^+$ | $4_2^+$ |
|---|---------|---------|---------|---------|---------|---------|
| 0 : (0,0)                               | 100     | 0       | 0       | 0       | 0       | 0       |
| 2 : (2,0)                               | 0       | 0       | 0       | 0       | 0       | 0       |
| 2 : (3,1)                               | 0       | 0       | 0       | 0       | 0       | 1       |
| 2 : (4,2)                               | 0       | 100     | 100     | 100     | 100     | 99      |

**Table 4.**  $SU(3)$  content of some low lying states with positive parity, given in percent, for the theoretical calculation which includes the mixing. The numbers are only approximate and not all irreps are shown. The  $n\hbar\omega$  denotes the shell excitation number.

| $n\hbar\omega (\lambda, \mu) / L_i^\pi$ | $1_1^-$ | $2_1^-$ | $3_1^-$ |
|---|---------|---------|---------|
| 1 : (2,1)                               | 100     | 100     | 100     |
| 3 : (3,0)                               | 0       | 0       | 0       |
| 3 : (4,1)                               | 0       | 0       | 0       |
| 3 : (5,2)                               | 0       | 0       | 0       |
| 3 : (6,3)                               | 0       | 0       | 0       |

**Table 5.**  $SU(3)$  content of some low lying states with negative parity, given in percent, for the theoretical calculation which includes mixing. The numbers are only approximate and not all irreps are shown. The  $n\hbar\omega$  denotes the shell excitation number.

structure, after applying a geometric mapping, results as default using simple symmetry arguments. Ignoring the PEP leads to a denser spectrum at low energy, as already shown for the case of  $^{12}\text{C}$  in [15]. As a result, the degeneracy obtained in [12] in some bands are not there at all. For example, the spin doublets in the (010E) and (001F) bands, predicted in the ACM, are broken and states are shifted to higher energy due to the implementation of the PEP.

The SACM can reproduce the experimental data well and for the transition values often better than in [12], even considering that it uses a phenomenological, algebraic Hamiltonian and not a microscopic interaction as used in [1, 2, 6]. The algebraic structure makes it easier to compare to [12] and also allows to retrieve more data.

In conclusion, one cannot ignore the PEP in  $^{16}\text{O}$ , otherwise it leads to a wrong understanding of the cluster structure. The SACM is able to describe well the structure of  $^{16}\text{O}$ , concerning the spectrum and several transition values. The ACM, in its present form, is not applicable to the cluster structure of light nuclei.

Finally, though density profiles show an approximate tetrahedral structure [32] and a classical treatment suggests a grouping of bands according to the  $T_4$  dynamical group, the antisymmetrization destroys it and requires a different grouping into bands. Also states of a  $T_4$  irrep are destroyed or shifted to higher energy. While the ACM works for atomic cluster molecules, it cannot be applied in its present form to nuclear cluster systems, until the PEP is taken into account.

## Acknowledgments

We acknowledge financial support from DGAPA-PAPIIT (IN100418) and CONACyT (project number 251817).

## Appendix

Here, we will construct a *geometrical* octupole oscillator model for  $^{16}\text{O}$ :

The Hamiltonian is given by

$$H = \hbar\Omega_3 \left( N + \frac{7}{2} \right) \quad , \quad (13)$$

where  $N$  is the number operator. The energy  $\hbar\Omega_3$  of the first vibrational state  $3_1^-$  can immediately be determined. The energy of this state is at 6.13 MeV [33], i.e

$$\hbar\Omega_3 = 6.13 \text{ MeV} \quad . \quad (14)$$

The geometrical quadrupole operator is to lowest order in  $\alpha_{30}$  given by

$$Q_{30} = \frac{3Ze}{4\pi} R_0^3 \alpha_{30} \quad , \quad (15)$$

where  $R_0 = 1, 2 A^{\frac{1}{3}}$  fm,  $e$  is the unit charge and  $\alpha_{30}$  is the deformation operator.

The  $B(E3; 3_1^- \rightarrow 0_1^+)$  value is given by

$$B(E3; 3_1^- \rightarrow 0_1^+) = \frac{1}{7} | \langle 0_1^+, 0 || Q_{30} || 0_1^-, 0 \rangle |^2 \quad , \quad (16)$$

where the "1" =  $(2J_f + 1)$ , with  $J_f = 0$  and "7" =  $(2J_i + 1)$ , with  $J_i = 3$ , the final and initial spin of the states.

For the calculation of the reduced matrix element, we define first the initial and final states, furthermore the quantization of the variable  $\alpha_{30}$ :

$$\begin{aligned} |i\rangle &= \mathbf{b}_{30}^\dagger |0\rangle \\ |f\rangle &= |0\rangle \\ \alpha_{30} &= \sqrt{\frac{\hbar}{2B_3\Omega_3}} (\mathbf{b}_{30}^\dagger + \mathbf{b}_{30}) \quad , \quad (17) \end{aligned}$$

with  $\mathbf{b}^{30} = \mathbf{b}_{30}$  and  $B_3$  is the mass parameter of the geometric theory.

With this, the matrix element of the quadrupole operator is

$$\begin{aligned} \langle f | Q_{30} | i \rangle &= \frac{3Ze}{4\pi} R_0^3 \sqrt{\frac{\hbar}{2B_3\Omega_3}} \\ &= \begin{pmatrix} 0 & 3 & 0 \\ 0 & 0 & 0 \end{pmatrix} \langle f || Q_3 || i \rangle \\ &= -\frac{1}{\sqrt{7}} \langle f || Q_3 || i \rangle \quad (18) \end{aligned}$$

( $R_0 = 1.2 A^{\frac{1}{3}}$ ). Therefore, the reduced matrix element is

$$\langle f || Q_3 || i \rangle = \frac{3Ze}{4\pi} R_0^3 \sqrt{\frac{\hbar}{2B_3\Omega_3}} (-\sqrt{7}) \quad . \quad (19)$$

Using the expression for the  $B(E3)$  value above and resolving for  $B_3c^2$  (using  $\frac{\hbar}{B_3\Omega_3} = \frac{(\hbar c)^2}{(B_3c^2)(\hbar\Omega_3)}$ ), we obtain

$$\begin{aligned} & -\sqrt{7} \left( \frac{3Ze}{4\pi} \right) R_0^3 \sqrt{\frac{(\hbar c)^2}{2(\hbar\Omega_3)}} \frac{1}{\sqrt{B_3c^2}} \\ & = 13.5 (0.05940 A^{\frac{4}{3}})^{\frac{1}{2}} e \text{ fm}^3 = 20.89 e \text{ fm}^3 \quad , \quad (20) \end{aligned}$$

where we use the experimental value 13.5 WU for the octupole transition on the right hand side and the factor in the parenthesis is the conversion from WU to  $e^2 \text{ fm}^4$ .

Plugging in the values and resolve for  $(Bc^2)$ , also using  $e^2 = 1.44 \text{ MeVfm}$ , we obtain the value

$$(B_3c^2) \approx 204555 \text{ MeVfm}^2 \quad . \quad (21)$$

Now we determine the value of  $\alpha_{30}$ , which gives the octupole deformation denoted by  $\beta_{30}$ , defined as

$$\begin{aligned} \beta_{30} = \alpha_{30} &= \langle f | \alpha_{30} | i \rangle = \sqrt{\frac{(\hbar c)^2}{2(B_3c^2)(\hbar\Omega_3)}} \\ &= 0.125 \quad , \quad (22) \end{aligned}$$

which gives the same as  $\langle f | (\alpha_{30})^2 | i \rangle$ .

## References

1. K. D. Launey, T. Dytrych and J. P. Draayer, Progr. in Part. and Nucl. Phys. **89** (2016), 101.
2. T. Dytrych, *Evidence for Symplectic Symmetry in ab initio no-core Shell Model Results*, (PhD Thesis, Louisiana State University, 2008).
3. P. Schuck, J. Phys.: Conf. Ser. **436** (2013), 012065
4. P. Schuck, Y. Funaki, H. Horiuchi, G. Röpke, A. Tohsaki and T. Yamada, Physica Scripta **91** (2016), 123001.
5. Y. Funaki, Phys. Rev. C **97** (2018), 021304(R).
6. A. Tohsaki, H. Horiuchi, P. Schuck and G. Röpke, Phys. Rev. Lett. **87** (2001), 192501.
7. M. Freer, Rep. Prog. Phys. **70** (2007) 2149.
8. M. Freer, H. Horiuchi, Y. Kanada-En'yo, D. Lee and U.-G. Meissner, Rev. Mod. Phys. **90** (2018), 03500.
9. Y. Funaki, M. Girod, H. Horiuchi, G. Röpke, P. Schuck, A. Tohsaki and T. Yamada, J. Phys. G: Nucl. Part. Phys. **37** (2010) 064012.
10. P. Schuck, AIP Conference Proceedings **2038** (2018), 020002
11. R. Bijker and F. Iachello, Phys. Rev. Lett. **112** (2014), 152501.
12. R. Bijker and F. Iachello, Nucl. Phys. A **957** (2017), 154.
13. D. J. Marín-Lámbarri, R. Bijker, M. Freer, et al., Phys. Rev. Lett. **113** (2014), 012502.
14. R. Bijker and F. Iachello, Ann. Phys. (N.Y.) **298** (2002), 334.
15. P. O. Hess, Eur. Phys. J. A **54** (2018), 32.
16. J. Cseh, Phys. Lett. B **281** (1992), 173.
17. J. Cseh and G. Lévai, Ann. Phys. (N.Y.) **230** (1994), 165.
18. F. Hoyle, Ap. J. Suppl. **1** (1954), 121.
19. K. Wildermuth and Y. C. Tang, *A Unified Theory of the Nucleus*, (Academic Press, New York, 1977).
20. V. C. Aguilera-Navarro, M. Moshinsky and P. Kramer, Ann. Phys. **54** (1969), 379.
21. M. Moshinsky and Y. Smirnoc. *The Harmonic Oscillator in Modern Physics*, (Harwood Academic Publishers, Australia, 1996).
22. E. Wigner, in *Group Theoretical Concepts and Methods in Elementary Particle Physics*, ed. by F. Gürsey., (Gordon and Breach, New York, 1964).
23. J.P. Draayer and Y. Akiyama, J. Math. Phys. **14** (1973), 1904.
24. D. J. Rowe and C. Bahri, J. Math. Phys. **41** (2000), 6544.
25. J. P. Elliott, Proc. R. Soc. London A **245**, (1958) 128; **245** (1958), 562.
26. D. J. Rowe, Rep. Prog. Phys. **48** (1985), 1419.
27. O. Castaños, J. P. Draayer and Y. Leschber, Z. f. Phys. **A329** (1988), 33.
28. J. Blomqvist and A. Molinari, Nucl. Phys. A **106** (1968), 545.
29. O. Castaños and J. P. Draayer, Nucl. Phys. A **491** (1989), 349.
30. O. Castaños, P. O. Hess, P. Rocheford and J. P. Draayer, Nucl. Phys. A **524** (1991), 469.
31. P. O. Hess, G. Lévai and J. Cseh, Phys. Rev. C **54** (1996), 2345.
32. Y. Kanada-En'yo, Phys. Rev. C **96** (2017), 034306.
33. www.nndc.bnl.gov/ensdf
34. H. Yépez-Martínez, M. J. Ermatamov, P. R. Fraser and P. O. Hess, Phys. Rev. C **86** (2012), 034309.
35. W. Greiner and J. M. Eisenberg, *Nuclear Theory I: Nuclear Models*, (North-Holland, Amsterdam, 1987).